JOURNAL OF CATALYSIS **166,** 16–24 (1997)
ARTICLE NO. CA971486

Catalytic Activity and Deactivation of SO_2 Oxidation Catalysts in Simulated Power Plant Flue Gases

S. G. Masters,* A. Chrissanthopoulos,† K. M. Eriksen,* S. Boghosian,† and R. Fehrmann*,[1]

*Department of Chemistry, Building 207, Technical University of Denmark, DK-2800 Lyngby, Denmark; and †Institute of Chemical Engineering and High Temperature Chemical Processes and Department of Chemical Engineering, University of Patras, P.O. Box 1414, GR-26500 Patras, Greece

Received November 28, 1995; revised August 15, 1996; accepted September 30, 1996

The catalyst deactivation and the simultaneous formation of compounds in commercial SO_2 oxidation catalysts have been studied by combined activity measurements and *in situ* EPR spectroscopy in the temperature range 350–480°C. The applied feed gas compositions were 0.2% SO_2, 4.5% O_2, 15% CO_2, and ~80% N_2; and 0.2% SO_2, 4% O_2, 7% H_2O, 14% CO_2, and ~75% N_2. These conditions simulate flue gas from coal fired power plants with and without water. It was shown that in both dry and wet flue gas, the V(IV) compound $K_4(VO)_3(SO_4)_5$ precipitates below the temperature of catalyst deactivation. However, for a given catalyst composition, the deactivation temperature in the wet flue gas was strongly influenced by the structure of the support, whereas similar behaviour was not observed in the dry flue gas. Thus, one of the studied catalysts, with a particular pore structure, most probably a V(III) compound, precipitated first during deactivation in the wet flue gas, while the V(IV) compound, $K_4(VO)_3(SO_4)_5$, only precipitated with a further lowering of the temperature. Water vapour seems therefore to have a significant influence on the performance of the SO_2-oxidation catalyst. A qualitative explanation is given for the formation of both V(IV) and V(III) compounds during deactivation.

INTRODUCTION

The industrial catalyst for SO_2 oxidation, which is the key process in the production of sulfuric acid, is well described during operating conditions by the molten-salt/gas model system $M_2S_2O_7/V_2O_5$–$SO_2/O_2/SO_3/N_2$, where M = Na, K, Cs, or a mixture of these (1, 2). The oxidation of SO_2 takes place at 440–460°C as a homogeneous reaction in the liquid phase of a molten salt mixture consisting of V_2O_5 dissolved in pyrosulfates and dispersed on an inert porous support of kieselguhr (3) and hence is a Supported Liquid Phase (SLP) catalyst. Fundamental technical problems in the production of sulfuric acid regarding catalyst performance at lower temperatures are still unsolved. The sudden loss of activity at temperatures below ~420°C remains, despite thorough research efforts, a major problem. This means that the actual working temperature of the catalyst must be 50°C higher than the temperature which would allow a 99.8% conversion of SO_2 in a once-through multi-bed reactor process and would thereby enable the elimination of the high-cost interstage absorption of SO_3.

The constant demand for abatement technologies including flue gas desulfurization processes has led to the development of several processes for SO_2 removal (4), which, however, are often sources of secondary pollution, generating e.g. wastewater, gypsum, or slurries. An exception is the so-called SNOX-process which involves catalytic oxidation of SO_2 into commercial grade sulfuric acid (4), whereby no waste is produced.

The operating conditions for the catalyst during flue gas desulfurization are rather different from those applied in conventional sulfuric acid production. This is partly because the SO_2 concentration is substantially lower (e.g., 0.1–0.2% SO_2 compared to 10% SO_2 in conventional sulfuric acid production). Moreover, the high water vapour content in the flue gas appears to be of utmost significance mostly due to its strong influence on the chemical composition of the catalyst (transformation of pyrosulfate into hydrogensulfate). This drastic change of the solvent may in turn influence the type of catalytically active complexes of vanadium in the melt.

By controlling the water vapour content in the feed gas, the influence of water on the catalytic activity for the SO_2 conversion can be visualized by Arrhenius plots of apparent reaction rates vs $1/T$. The most important feature of the Arrhenius plot is a break occurring at a specific temperature, thus leading to a sharp increase of the apparent activation energy (5–8). It is now well established (5, 9–12, 13) that this decrease in catalyst activity during dry conditions of conventional sulfuric acid production is due to the precipitation of crystalline V(III), V(IV), and mixed valence V(IV)–V(V) compounds, whereby the vanadium complex equilibrium is shifted away from the active V(V) species. The compounds $Na_2VO(SO_4)_2$, $K_4(VO)_3(SO_4)_5$,

[1] To whom correspondence should be addressed. E-mail: rf@kemi.dtu.dk.

0021-9517/97 $25.00

$K_6(VO)_4(SO_4)_8$, $Cs_2(VO)_2(SO_4)_3$, $NaV(SO_4)_2$, $KV(SO_4)_2$, $CsV(SO_4)_2$, and β-$VOSO_4$ (5, 13) have all been identified as deactivation products. The present work is the first to be published on investigations of SO_2 removal over industrial sulfuric acid catalysts in simulated flue gases. Magnetic resonance spectroscopy, EPR for the study of the reduced catalysts and NMR for the study of the oxidized catalysts, is probably the only useful method for *in situ* studies of these supported catalysts since the spectra can be obtained without interference from the solid carrier.

EXPERIMENTAL

Catalysts

The commercial catalysts investigated were VK-WSA, VK38, and VK58, manufactured by Haldor Topsøe A/S, Denmark. The VK-WSA is applied in the flue gas desulfurization process and has the same chemical composition as VK38 (molar ratio K/Na/V = 3/0.8/1, V_2O_5 = 6.5% w/w) but a smaller average pore-size of the support. The VK58 catalyst has a modified chemical composition (molar ratio K/Cs/Na/V = 3/1/0.25/1) including Cs in addition to K and Na as promoters. The catalyst pellets were crushed to a size of 1–1.5 mm and placed in the flow reactor or in the high-temperature EPR cavity cell, as described in (5, 9, 13).

Flue Gas Generation System

Feed gas with a composition similar to dry flue gas (without NO_x) was prepared by mixing SO_2 (>99.9%), O_2 (99.8% O_2, 0.2% Ar + N_2), CO_2 (>99.7%), and N_2 (<40 ppm $H_2O + O_2$) either by individual flowmeters (5) or by premixing the gases in an evacuated special steel gas bottle followed by external heating at the bottom to obtain a uniform gas mixture by convection. A flow diagram is shown in Fig. 1. The absence of NO_x corresponds to the condition of the SO_2 oxidation in the SNOX-process where NO_x is removed upstream (4). The SO_2 concentration was monitored by UV-spectrophotometry on a Perkin–Elmer Lambda-9 or a Hitachi U3000 spectrophotometer, using a gas cuvette (quartz Suprasil, Hellma GmbH) with a path length of 100 mm. The concentrations of O_2, CO_2, and N_2 were checked by gas chromatography on a Shimadzu GC-8APT chromatograph equipped with Supelco Chromosorb 102 or 5Å molecular sieve columns.

Wetting of the flue gas was achieved by bubbling the dry gas to saturation through water which was contained in two flasks connected in series and immersed in a thermostat controlled at the appropriate temperature. With a thermostat temperature of 40°C a 7% water vapour content was achieved. The water vapour concentration was measured by a Jenway 5075 humidity meter. All 1/8″ stainless steel tubes in the experimental setup were heated to 80–90°C by wrapped heating tape in order to prevent condensation.

EPR and Catalytic Activity Setup

For the activity measurements and compound isolation, the gases were led (Fig. 1) to a molten salt reactor made of Pyrex glass. The reactor cell was mounted in a double-walled canthal-wire-wound quartz-tube furnace (5). The temperature was controlled to within ±2°C and measured by a chromel–alumel thermocouple placed at the reactor cell area containing the catalyst sample. The reactor exit gas stream was passed through stainless steel tubes to a SO_3 trap made of borosilicate glass and placed in an antifreeze bath at −35°C cooled by an immersion cooler before flowing to the spectrophotometer. Here the SO_2 conversion was monitored by on-line UV-spectrophotometry, and the conversion was always below 15%. Thus the reactor could be considered differential.

For the EPR investigations, a setup almost identical to that described above was used, but the SO_3 cooling trap was replaced with an acid absorber of 98% w/w sulfuric acid. The flue gas was led to a quartz reactor flow cell as described in detail in (9) which fits into a Bruker ER4114HT high-temperature X-band cavity mounted in a slightly modified JEOL-JES-ME 1X EPR spectrometer connected to a PC-based acquisition system. The temperature was measured by a 1-mm nonmagnetic chromel-constantan thermocouple placed in contact with the catalyst bed. The field calibration was performed with an external Mn(II)-standard and, to correct the signal intensity for the temperature dependence, an internal separate ruby crystal was applied. The space velocity was adjusted to be in the range 5000–10000 h^{-1}, so the conversion over the catalyst bed was always below 15%.

RESULTS AND DISCUSSION

Catalytic Activity

The three catalysts investigated are all designed for use in the manufacturing of sulfuric acid. The same type of catalyst is also used for flue gas desulfurization and therefore the chemical composition is probably not optimized for the flue gas cleaning process. The VK38 type is a general purpose catalyst promoted by both Na and K and is to be used in a wide range of beds and environments. VK58 is an advanced, typical last bed catalyst promoted by a mixture of Na, K, and Cs. The VK-WSA catalyst, although chemically identical to VK38, is designed specifically for use in humid gases with a modified porous support of kieselguhr. The specifications of the catalyst can be seen in Table 1.

The performance of the catalysts in both wet and dry simulated flue gas in the temperature range 350–470°C can be seen in the Arrhenius plots of Fig. 2. The wet flue gas consists of 0.2% SO_2, 4% O_2, 7% H_2O, 14.1% CO_2, and 74.8% N_2,

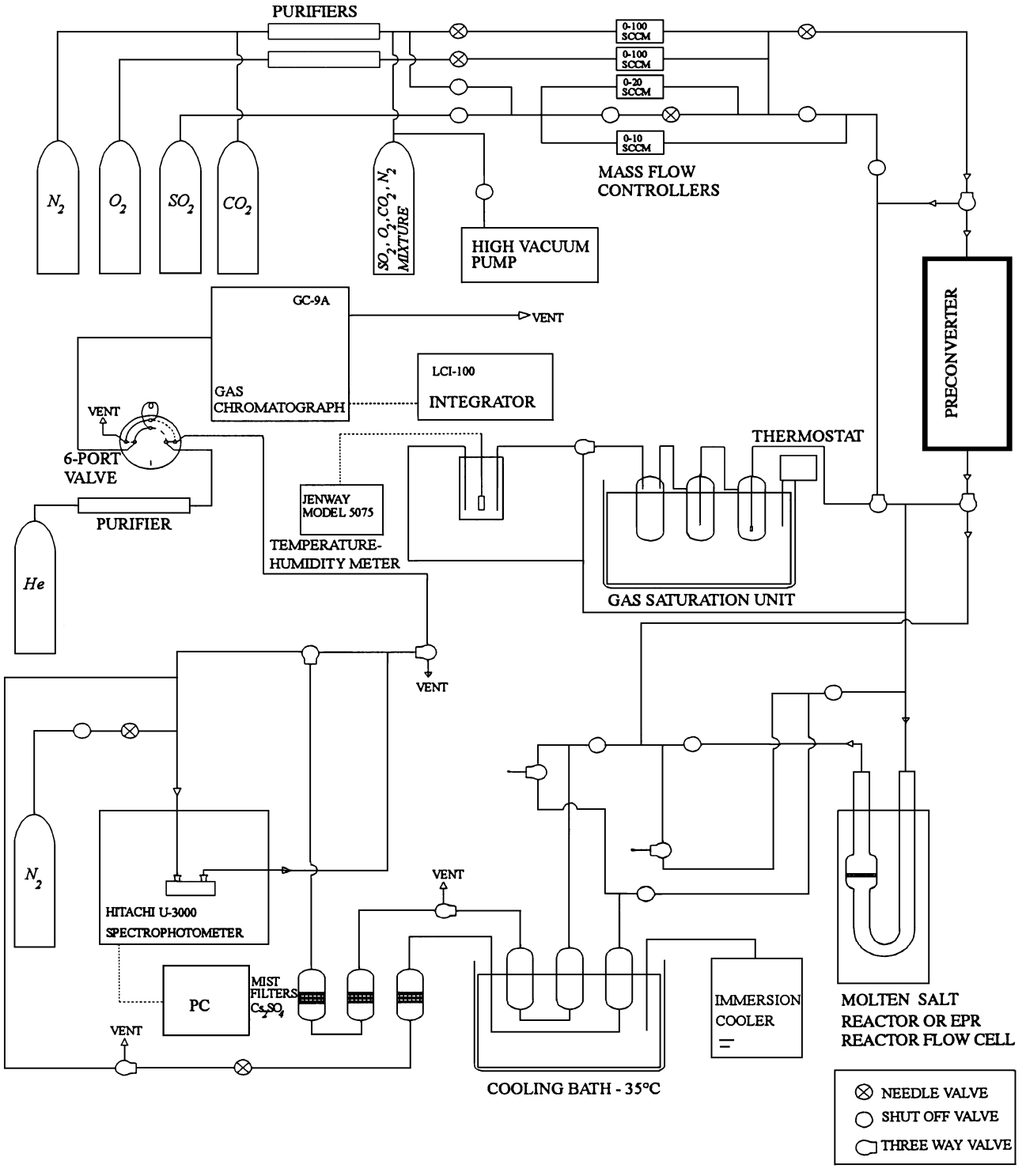

FIG. 1. Flow diagram of the experimental setup.

and the dry flue gas of 0.2% SO_2, 4.5% O_2, 15.1% CO_2, and 80.2% N_2. Besides obvious differences in activity, all curves exhibit the same features: in the high temperature region an apparent activation energy of around 75 kJ/mol is found. However, at a certain temperature (breakpoint temperature, T_b) a steep decrease in the activity is observed, leading to an apparent activation energy of ca. 230 kJ/mol. The apparent activation energies above and below the deactivation temperature are in good agreement with previous investigations on model melts and supported catalysts

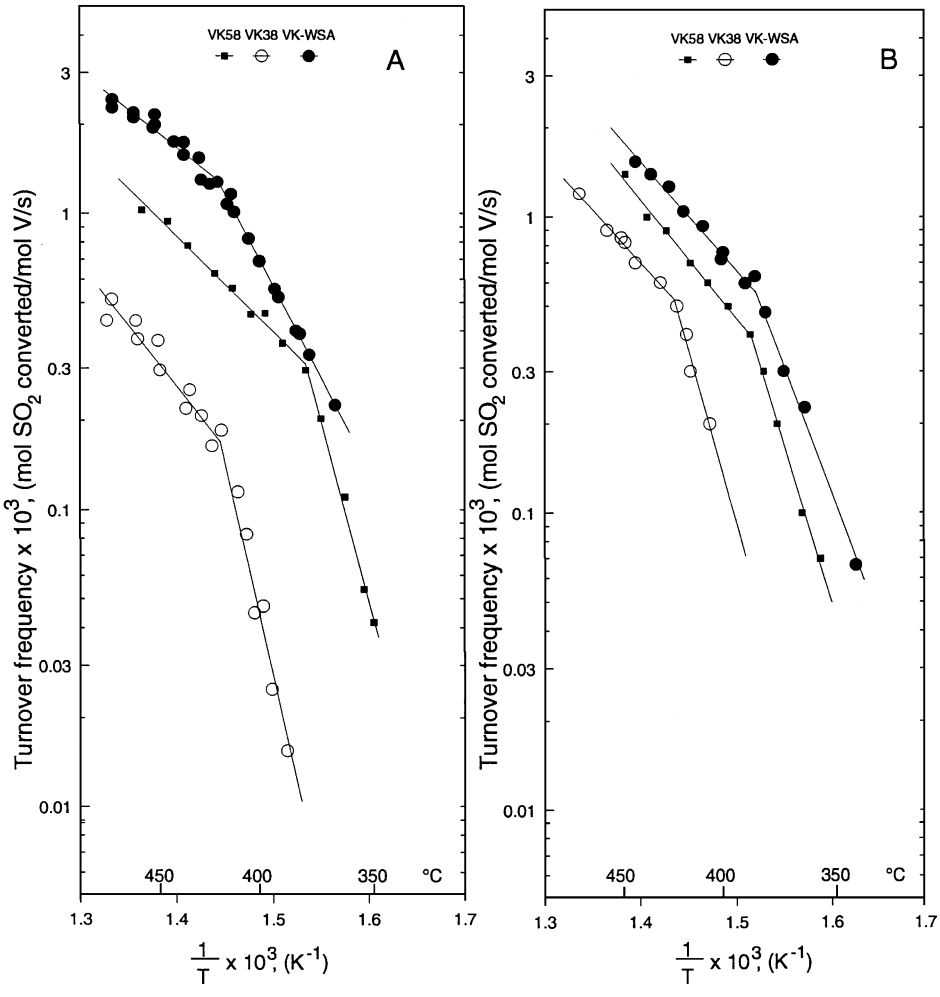

FIG. 2. Arrhenius plots for industrial sulfuric acid catalysts in (A) 0.2% SO_2, 4.5% O_2, 15.1% CO_2, and 80.2% N_2 (dry flue gas) and in (B) 0.2% SO_2, 4.0% O_2, 7.0% H_2O, 14.0% CO_2, and 74.8% N_2 (wet flue gas).

(5, 7, 11, 15–17). Earlier investigations of similar catalysts in unconverted sulfuric acid synthesis gas (i.e., 10% SO_2, 11% O_2, and 79% N_2) have shown that this drop in activity can be attributed to precipitation of crystalline compounds of vanadium in the oxidation state III and/or IV (5, 9, 13). The actual breakpoint temperatures are listed in Table 1. It should be noted that the T_b of both VK38 and VK58 is unaffected by the water vapour content, whereas in the case of VK-WSA, T_b decreases by 30°C in the presence of water vapour. It is remarkable that the structure of the support has such an influence, but the desired deactivation temperature below 350°C is still not reached.

With respect to the activity in the high temperature region, Fig. 2 shows that both VK58 and VK-WSA seem almost unaffected by the water vapour content, whereas VK38 performs rather poorly in the dry gas. As previously stated in (5), it should be noted that the turnover frequencies displayed in Fig. 2 are only relative and not the highest attainable.

In Situ EPR Spectroscopy

In situ EPR spectroscopy is one of the few direct methods available to follow the content of V(IV) in operating catalysts, since only the paramagnetic $[Ar]3d^1$ V(IV) species are detectable. Thus V(V) ($[Ar]3d^0$) is diamagnetic and V(III) ($[Ar]3d^2$) resonates far from the field applied here due to the zero field splitting of the electronic spin state. Earlier EPR investigations (9) have shown that the inert support of kieselguhr is also EPR silent. *In situ* EPR spectroscopy has previously been shown to be useful for monitoring the catalyst deactivation in sulfuric acid synthesis gas (9, 13).

The EPR spectra of the three catalysts in the two gas types can be seen in Figs. 3–5. In all cases a very broad isotropic line is observed at high temperature, $g_{avg} \approx 2.01$ and $\Delta B_{pp} \approx 200$–$500$ G. Such high g-values have earlier (9, 13, 14) been observed by us and others (10) for the broad line at these temperatures, but similar high values around $g = 2.0$ can also be found (18) for other VO^{2+}

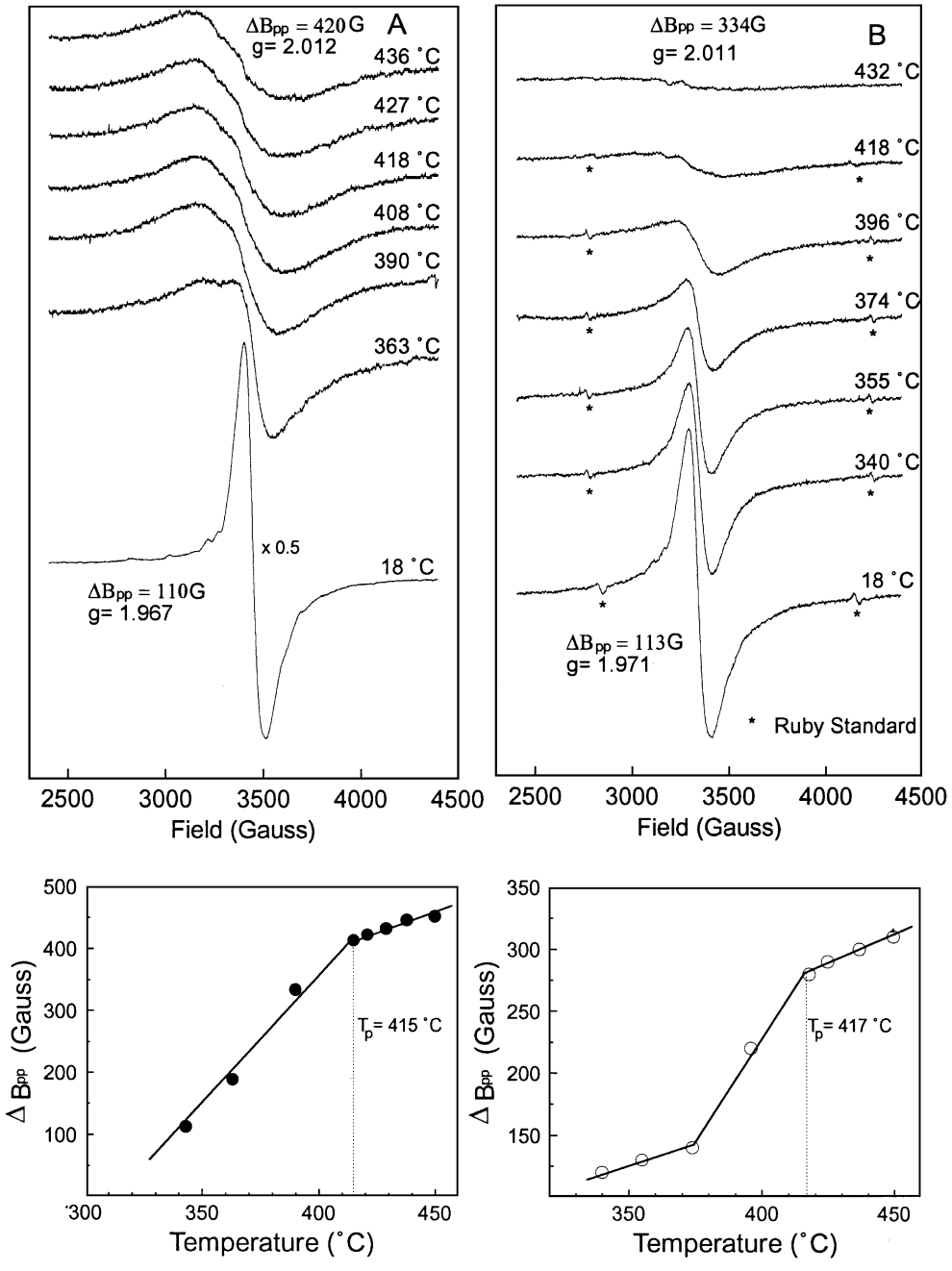

FIG. 3. EPR spectra of VK38 catalyst at various temperatures in (A) 0.2% SO_2, 4.5% O_2, 15.1% CO_2, and 80.2% N_2 (dry flue gas) and in (B) 0.2% SO_2, 4.0% O_2, 7.0% H_2O, 14.0% CO_2, and 74.8% N_2 (wet flue gas). For convenience the signal intensity of the spectrum measured at the lowest temperature in (A) has been reduced by the indicated factor. Insert: Apparent line width (ΔB_{pp}) vs temperature. The dotted line represents the temperature T_p where a marked change in the linear relationship is observed.

complexes. Since the conversion is low over the catalyst bed, the V(IV) concentration is relatively high and the broad isotropic line is therefore attributed to dissolved dimeric and/or polymeric V(IV) complexes where spin coupling between neighboring V atoms gives rise to a multiline spectrum (13). This phenomenon has previously been observed (19–21) for dimeric V(IV) complexes at room temperature where a badly resolved 15-line spectrum superimposed on a broad central line was found. At high temperature this pattern is expected to be even less resolved for dimers and for polymeric complexes, the long-range coupling making the hyperfine structure undetectable. The very weak half-field peak (at ~1700 G) found for the forbidden ($\Delta m_s = \pm 2$) transition in some solid V^{4+} dimers (22) has not been

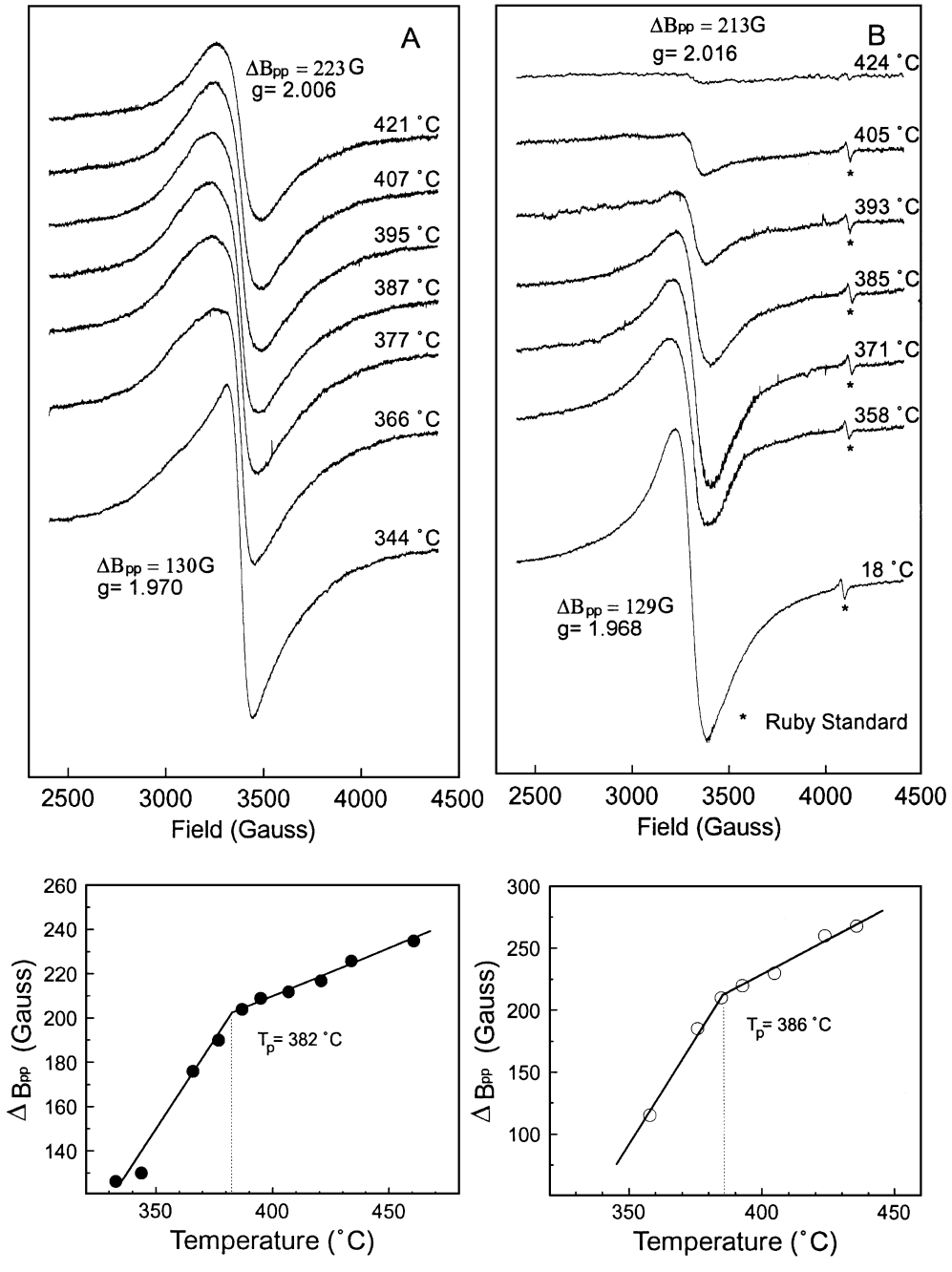

FIG. 4. EPR spectra of VK58 catalyst at various temperatures in (A) 0.2% SO_2, 4.5% O_2, 15.1% CO_2, and 80.2% N_2 (dry flue gas) and in (B) 0.2% SO_2, 4.0% O_2, 7.0% H_2O, 14.0% CO_2, and 74.8% N_2 (wet flue gas). Insert: Apparent line width (ΔB_{pp}) vs temperature. The dotted line represents the temperature T_p where a marked change in the linear relationship is observed.

detected by us at low field in spectra obtained from samples and conditions similar to those for Figs. 3–5. However, this does not exclude the possible presence of dimers (eventually in equilibrium with polymeric V(IV)) since the high temperature and the dissolved state for the species may lead to weakening and broadening of the spectra and the disappearance of the 15-line feature of the central signal for V^{4+} dimers (21).

Below a certain temperature, called T_p, the dependence of the apparent line width ΔB_{pp} of the spectra in Figs. 3–5 undergoes a marked change, except for the VK-WSA catalyst in the wet flue gas (Fig. 5B). The spectra at the lowest temperatures exhibit some anisotropy, but their isotropic *g*-values and linewidths are close to what has been found previously for the V(IV) compound $K_4(VO)_3(SO_4)_5$, which is known to cause deactivation of catalysts in the traditional

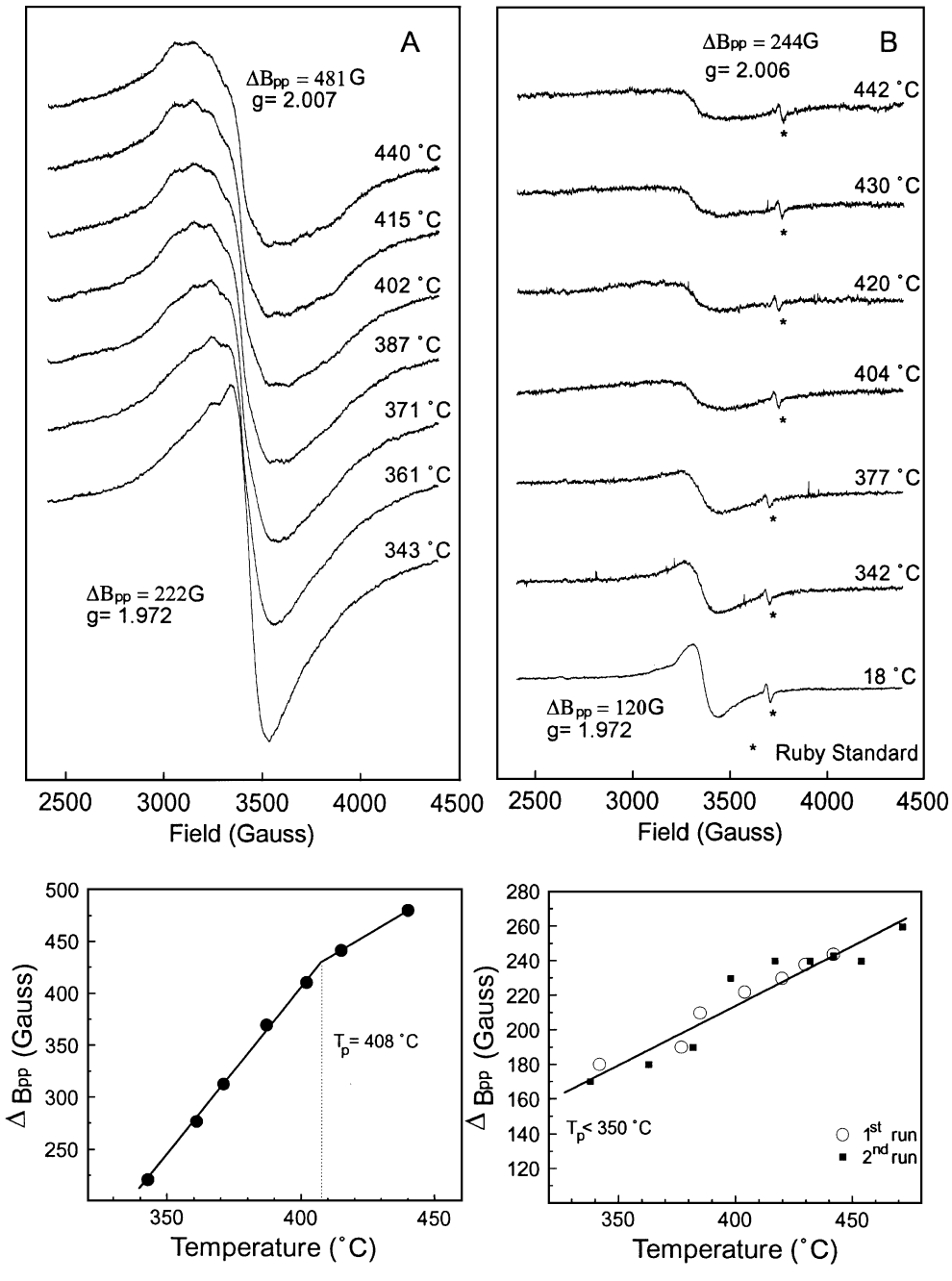

FIG. 5. EPR spectra of VK-WSA catalyst at various temperatures in (A) 0.2% SO_2, 4.5% O_2, 15.1% CO_2, and 80.2% N_2 (dry flue gas) and in (B) in 0.2% SO_2, 4.0% O_2, 7.0% H_2O, 14.0% CO_2, and 74.8% N_2 (wet flue gas). Insert: Apparent line width (ΔB_{pp}) vs temperature. The dotted line represents the temperature T_p where a marked change in the linear relationship is observed.

gas for sulfuric acid production (5, 9, 13). Thus this compound probably starts to precipitate at the temperature T_p listed in Table 1. Since ΔB_{pp} is obviously an average value influenced by several lines, these plots should only be taken as an empirical way to obtain the temperature of precipitation, T_p. The error in ΔB_{pp} is estimated to be 10–20% relatively and is highest for the broadest lines obtained at high temperature. T_b and T_p coincide fairly well in all series except for the VK-WSA catalyst in the wet flue gas. This is an indication that the loss of the catalytic activity is usually caused by depletion of the catalytic active vanadium species, due to precipitation of crystalline V(IV) compounds. Such a deactivation process is expected to be reversible. This is in agreement with the industrial experience that upon reheating the catalyst the activity is regained (6), and where the hysteresis behaviour observed

TABLE 1

Temperature of Deactivation and Precipitation for Industrial Sulfuric Acid Catalysts

Catalyst	Chemical composition (molar)	Average pore size	T_b (°C)[a]	T_p (°C)[b]
VK38[c]	K/Na/V = 3/0.8/1	normal	422	415
VK58[c]	K/Cs/Na/V = 3/1/.25/1	normal	379	382
VK-WSA[c]	K/Na/V = 3/0.8/1	small	419	408
VK38[d]	K/Na/V = 3/0.8/1	normal	422	417
VK58[d]	K/Cs/Na/V = 3/1/.25/1	normal	384	386
VK-WSA[d]	K/Na/V = 3/0.8/1	small	387	340–350

[a] T_b is the temperature at which the breakpoint in the Arrhenius plots and the compound precipitation (V(IV) and/or V(III)) occur simultaneously.

[b] T_p is the temperature at which precipitation of crystalline V(IV)-compounds occurs as detected by EPR.

[c] Feed gas: 0.2% SO_2, 4.5% O_2, 15% CO_2, and ~80% N_2.

[d] Feed gas: 0.2% SO_2, 4% O_2, 7% H_2O, 14% CO_2, and ~75% N_2.

is probably due to the necessary thermal decomposition of the inactive low-valence vanadium compounds into active V(V) complexes in solution, at relatively high temperature (5, 9, 13, 14). The observed hysteresis behaviour means that diffusion limitation as the reason for the breakpoint and deactivation is very unlikely.

The VK-WSA catalyst in wet flue gas represents a special case since several runs have shown a "delay" of the V(IV) precipitation compared to the activity drop, i.e., it appears at a lower temperature than T_b. The EPR signal intensity also seems surprisingly weak (Fig. 5B). Double integration of the EPR spectra was performed and the result is shown in Fig. 6 for (B) two runs in wet and (A) one run in dry flue gas. The maximum of the V(IV) concentration for the VK-WSA catalyst in wet gas (Fig. 6B) is probably found close to the breakpoint temperature of the Arrhenius plot, $T_b = 387$°C. If V(IV) had precipitated below this temperature an *increase* of the integrated EPR signal of both solid and liquid V(IV) would have been observed, also below T_b. This behaviour is shown in Fig. 6A for the catalyst in dry flue gas (Fig. 5A), for which T_b and T_p coincide fairly well. Hence the decrease (Fig. 6B) below T_b is probably due to the precipitation of an EPR silent V(III) compound whereby the concentration of V(IV) (and V(V)) in the solution is decreased due to the coupled redox equilibria V(III) $\rightleftarrows$ V(IV) $\rightleftarrows$ V(V) of the complexes in solution. Around 345°C, precipitation of the V(IV) compound has commenced, judging by the features of the EPR spectra. Therefore the relative V(IV) amount increases again until it becomes constant at around 290°C (spectra not shown in Fig. 5). Below 290°C the catalyst melt becomes totally solid.

Qualitatively, these observations might be explained by a marked difference in concentration and solubility of the V(III) and V(IV) compounds versus the temperature. Thus the V(III) compound has a considerably lower solubility than the V(IV) compound, judging from previous spectrophotometric measurements. Two scenarios are then possible:

(i) Normally, the equilibrium between V(III) and V(IV) is shifted to the V(IV) side, which means that the solubility limit of V(IV) will be reached at a higher temperature than that of V(III), resulting in precipitation of the V(IV) compound. At this particular temperature, T_1, the first V(IV) crystals are formed, causing a drop in the concentration of V(III) due to the coupled equilibrium system. If the temperature is further reduced, V(III) might reach its solubility limit too (at the temperature T_2), and a V(III) compound will also precipitate.

(ii) If, on the other hand, the V(III)–V(IV) equilibrium is shifted towards V(III), compounds of this oxidation state will precipitate first on decreasing the temperature to T_1. Below T_1 the concentration of V(IV) then decreases until its solubility limit is eventually reached at T_2. From T_2 to T_{fus}, V(III)- and V(IV)-precipitates coexist.

Scenarios like (i) and (ii) can now explain the shapes of the curves in Fig. 6 and the previous finding of both blue (V(IV)) and green (V(III)) crystalline compounds precipitated during the deactivation of the catalyst model

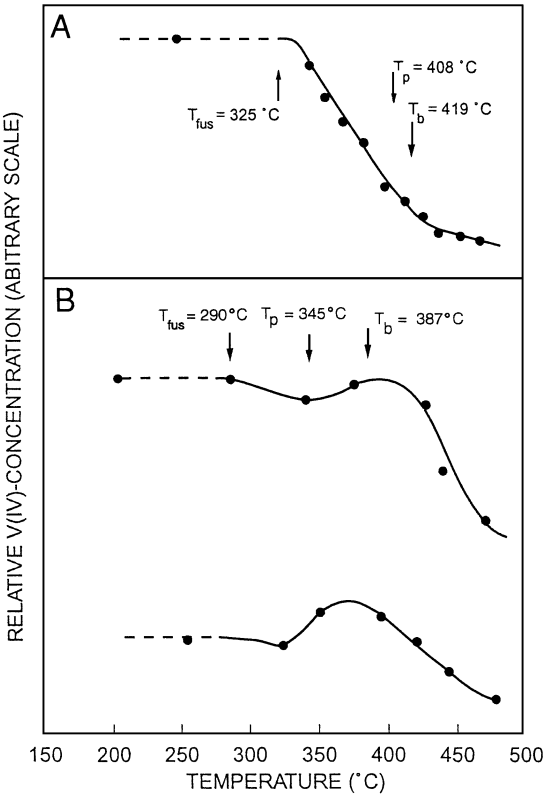

FIG. 6. Relative V(IV) concentration versus temperature for VK-WSA in (A) dry flue gas and in (B) wet flue gas (two runs). Constant level indicates T_{fus} while values for T_p and T_b are taken from Table 1.

melts in the sulfuric acid synthesis gas (5) and in the wet flue gas.

Thus, by the activity measurements, only T_1 is normally observed (as T_b) since the turnover frequency of SO_2 becomes unmeasurably low before T_2 is reached. By EPR spectroscopy, it is the temperature T_p, where precipitation of crystalline V(IV) compounds commences, that is registered. Thus T_p coincides with T_b when V(IV) compounds precipitate first. However, as demonstrated above (Fig. 6), it is possible to obtain an indication of T_b by EPR alone even when EPR silent compounds precipitate first.

It still remains to explain why the V(III)–V(IV) equilibrium shifs towards V(III), in the case of the VK-WSA catalyst, but not in the case with the other catalysts in the wet flue gas. Presumably the smaller pores of the VK-WSA carrier suppress the growth of V(IV) crystalline compounds. It is less surprising that this happens in the wet flue gas because the formation of hydrogensulfate due to the reaction $S_2O_7^{2-} + H_2O \rightleftarrows 2HSO_4^-$ is favored by the increasing partial pressure of water and the decreasing temperature (23), whereby the oxidation of V(III) by $S_2O_7^{2-}$ to V(IV) is suppressed. Therefore V(III) compounds might precipitate before the V(IV) compounds and cause deactivation of the VK-WSA catalyst in the wet flue gas.

Deactivation products (i.e., crystalline compounds) precipitated in the small pores of the catalyst cannot be isolated. Attempts to isolate and characterize deactivation compounds formed in unsupported model melt systems $M_2S_2O_7/V_2O_5$–$SO_2/SO_3/O_2/H_2O/CO_2/N_2$, where $M =$ Na, K, Cs, are in progress (24).

ACKNOWLEDGMENTS

This investigation has been supported by the EU programs BRITE-EURAM II (Contract BRE2.CT93.0447) and Human Capital and Mobility (Contract ERBCHBGCT920129) and the Danish Natural Science Research Council. The EU exchange program (ERASMUS) has supported the visit in the period March–June 1993 of S. G. Masters to the University of Patras, Greece. D. A. Karydis is thanked for experimental assistance and helpful discussions.

REFERENCES

1. Frazer, J. H., and Krikpatrick, W. J., *J. Am. Chem. Soc.* **62**, 1659 (1940).
2. Topsøe, H. F. A., and Nielsen, A., *Trans. Dan. Acad. Tech. Sci.* **1**, 18 (1947).
3. Kenney, C. N., *Catal. Rev.-Sci. Eng.* **17**, 203 (1975).
4. Smith, D. J., *Power Eng. Int.* (Apr. 21, 1994).
5. Boghosian, S., Fehrmann, R., Bjerrum, N. J., and Papatheodorou, G. N., *J. Catal.* **119**, 121 (1989).
6. Villadsen, J., and Livbjerg, H., *Catal. Rev.-Sci. Eng.* **17**, 203 (1978).
7. Boreskov, G. K., Polyakova, L. P., Ivanov, A. A., and Mastikhin, V. M., *Dokl. Akad. Nauk. SSSR* **210**, 626 (1973).
8. Grydgaard, P., Jensen-Holm, H., Livbjerg, H., and Villadsen, J., *ACS Symp. Ser.* **65**, 582 (1978).
9. Eriksen, K. M., Fehrmann, R., and Bjerrum, N. J., *J. Catal.* **132**, 263 (1991).
10. Mastikhin, V. M., Polyakova, G. M., Zyulkovski, Y., and Boreskov, G. K., *Kinet. Katal.* **11**, 1463 (1970); *Kinet. Catal.* **11**, 1219 (1971) [Engl. Transl.].
11. Doering, F. J., and Berkel, D., *J. Catal.* **103**, 126 (1987).
12. Doering, F. J., Yuen, H. K., Berger, P. A., and Unland, M. L., *J. Catal.* **104**, 186 (1987).
13. Eriksen, K. M., Karydis, D. A., Boghosian, S., and Fehrmann, R., *J. Catal.* **155**, 32 (1995).
14. Oehlers, C., Fehrmann, R., Masters, S. G., Eriksen, K. M., Sheinin, D. E., Balzhinimaev, B. S., and Elokhin, V. I., *Appl. Catal.* **147**(1), 127 (1996).
15. Mars, P., and Maessen, J. G. H., *in* "Proceedings 3rd International Congress on Catalysis, Amsterdam, 1964," Vol. 1, p. 266, Wiley, New York, 1965; *J. Catal.* **10**, 1 (1968).
16. Xie, K. C., and Nobile, A. J., *J. Catal.* **94**, 323 (1985).
17. Livbjerg, H., and Villadsen, J., *Chem. Eng. Sci.* **27**, 21 (1972).
18. Selbin, J., *Chem. Rev.* **65**, 153 (1965).
19. Belford, R. L., Chasteen, N. D., So, H., and Tapscott, R. E., *J. Am. Chem. Soc.* **91**, 4675 (1969).
20. Toftlund, H., Larsen, S., and Murray, K. S., *Inorg. Chem.* **30**, 3964 (1991).
21. Dickinson, L. C., Dunhill, R. H., and Symons, M. C. R., *J. Chem. Soc. A*, 922 (1970).
22. Abi-Aad, E., Bennani, A., Bonnelle, J.-P., and Aboukaïs, A., *J. Chem. Soc. Faraday Trans.* **91**, 99 (1995).
23. Fehrmann, R., Hansen, N. H., and Bjerrum, N. J., *Inorg. Chem.* **22**, 4009 (1983).
24. Nielsen, K., Fehrmann, R., Eriksen, K. M., Boghosian, S., Masters, S. G., and Chrissanthopoulos, A., manuscript in preparation.